Redox Biology 63 (2023) 102731

Contents lists available at ScienceDirect

Redox Biology

journal homepage: www.elsevier.com/locate/redox

The contribution of glutathione peroxidases to chloroplast redox homeostasis in Arabidopsis

Azahara Casatejada, Leonor Puerto-Galán, Juan M. Pérez-Ruiz *, Francisco J. Cejudo *

Instituto de Bioquímica Vegetal y Fotosíntesis, Universidad de Sevilla and CSIC, Avda. Américo Vespucio 49, 41092-Sevilla, Spain

ARTICLE INFO

Keywords:
Arabidopsis
Chloroplast
Glutathione peroxidase
NTRC
Peroxiredoxin
Thioredoxin

ABSTRACT

Oxidizing signals mediated by the thiol-dependent peroxidase activity of 2-Cys peroxiredoxins (PRXs) plays an essential role in fine-tuning chloroplast redox balance in response to changes in light intensity, a function that depends on NADPH-dependent thioredoxin reductase C (NTRC). In addition, plant chloroplasts are equipped with glutathione peroxidases (GPXs), thiol-dependent peroxidases that rely on thioredoxins (TRXs). Despite having a similar reaction mechanism than 2-Cys PRXs, the contribution of oxidizing signals mediated by GPXs to the chloroplast redox homeostasis remains poorly known. To address this issue, we have generated the Arabidopsis (*Arabidopsis thaliana*) double mutant *gpx1gpx7*, which is devoid of the two GPXs, 1 and 7, localized in the chloroplast. Furthermore, to analyze the functional relationship of chloroplast GPXs with the NTRC-2-Cys PRXs redox system, the *2cpab-gpx1gpx7* and *ntrc-gpx1gpx7* mutants were generated. The *gpx1gpx7* mutant displayed wild type-like phenotype indicating that chloroplast GPXs are dispensable for plant growth at least under standard conditions. However, the *2cpab-gpx1gpx7* showed more retarded growth than the *2cpab* mutant. The simultaneous lack of 2-Cys PRXs and GPXs affected PSII performance and caused higher delay of enzyme oxidation in the dark. In contrast, the *ntrc-gpx1gpx7* mutant combining the lack of NTRC and chloroplast GPXs behaved like the *ntrc* mutant indicating that the contribution of GPXs to chloroplast redox homeostasis is independent of NTRC. Further supporting this notion, *in vitro* assays showed that GPXs are not reduced by NTRC but by TRX *y*2. Based on these results, we propose a role for GPXs in the chloroplast redox hierarchy.

1. Introduction

Chloroplasts, the organelles that perform photosynthesis, are the factories of metabolic intermediates that support plant growth and development. However, because photosynthesis involves the transport of electrons in the presence of oxygen, it is a process that inevitably generates as by-products reactive oxygen species (ROS), which include superoxide, hydrogen peroxide, singlet oxygen, and hydroxyl radicals [1–3]. ROS have high reactivity with lipids, proteins, and nucleic acids; hence, their accumulation may cause damage to cell structures and, eventually, cell death [4]. In addition to this harmful effect, ROS have an important signaling function, which is essential for plant development and response to the environment [3,5–7]. Therefore, besides producing metabolic intermediates, chloroplasts are as well an important source of ROS in photosynthetic plant cells, the levels of which vary when plants undergo stressful environmental conditions, hence having an important signaling function in plant acclimation to the environment [1,8].

Plant growth and development depend on photosynthetic performance, which needs a strict balance between chloroplast ROS production and scavenging. This balance is maintained by non-enzymatic antioxidants such as carotenoids, ascorbate, and glutathione [9], and enzymatic antioxidants including a set of enzymes that show ROS scavenging activity. Among these enzymes, plant chloroplasts are equipped with superoxide dismutases that catalyze the conversion of superoxide to hydrogen peroxide [10]. The reduction of hydrogen peroxide is performed by two types of peroxidases, ascorbate peroxidases (APXs), of which the organelle harbors two isoforms localized at the stroma and the thylakoid, and thiol-dependent peroxidases (TPXs) including peroxiredoxins (PRXs) and glutathione peroxidases (GPXs) [11–14]. The gene family encoding PRXs in *Arabidopsis thaliana* is composed of 10 genes [15,16]. Depending on the reaction mechanism and enzyme structure, plant PRXs are classified into 1-Cys PRXs, which

Abbreviations: FDX, ferredoxin; FTR, ferredoxin-dependent thioredoxin reductase; FNR, ferredoxin NADP reductase; GPX, glutathione peroxidase; NTRC, NADPH-thioredoxin reductase; PRX, peroxiredoxin; RCA, Rubisco activase; TRX, thioredoxin.

* Corresponding authors. Instituto de Bioquímica Vegetal y Fotosíntesis, Universidad de Sevilla and CSIC, Avda. Américo vespucio 49, Sevilla 41092, Spain.
E-mail addresses: jperez4@us.es (J.M. Pérez-Ruiz), fjcejudo@us.es (F.J. Cejudo).

https://doi.org/10.1016/j.redox.2023.102731
Received 28 March 2023; Received in revised form 20 April 2023; Accepted 3 May 2023
Available online 22 May 2023

contain a single cysteine at the active site, and 2-Cys PRXs, containing two cysteine residues, peroxidatic and resolving, at their active site [14,15]. 2-Cys PRXs are further grouped as atypical 2-Cys PRXs, which are monomeric, hence containing the peroxidatic and resolving cysteines in a single polypeptide, and typical 2-Cys PRXs, homodimeric enzymes with the two subunits arranged in a head-to-tail conformation in which the peroxidatic and resolving cysteines are in different subunits [15,17]. In plant cells, the chloroplast is the organelle with the highest contents of 2-Cys PRXs; in the case of Arabidopsis, chloroplasts contain two almost identical typical 2-Cys PRXs, A and B, which are among the most abundant proteins in the stroma [18], and atypical PRX IIE and PRX Q [15].

Concerning the other class of TPXs, the Arabidopsis genome contains 8 genes encoding GPXs that show ubiquitous localization in different cell compartments, of which GPX1 and GPX7 are localized in the chloroplast [14,19,20]. Unlike GPXs from animal cells, the plant enzymes contain cysteine, not seleno-cysteine, and are more efficiently reduced by thioredoxin (TRX) than by glutathione [21,22]. Thus, the activity of GPXs and PRXs is highly interconnected to the TRX redox network, which in plant chloroplasts is composed by more than 20 isoforms including TRXs and TRX-like proteins [23–28]. It is well-established by *in vitro* analyses that chloroplast dimeric 2-Cys PRXs are reduced by different TRXs including classical TRXs of the types *m*, *f*, *x* and *y* [29–31], and TRX-like proteins such as TRX L2 [32], cold-drought stress protein of 32 kDa (CDSP32) [33] and atypical Cys His-rich TRX (ACHT) namely ACHT1 [34] and ACHT4 [35]. However, 2-Cys PRXs are more efficiently reduced by NADPH-dependent TRX reductase C (NTRC) [36–39]. Moreover, it was found that the severe growth inhibition phenotype of the Arabidopsis *ntrc* mutant, which is a knockout for NTRC, is suppressed by decreased contents of 2-Cys PRXs [40], showing the tight functional relationship of these enzymes and emphasizing the key role of 2-Cys PRX-dependent oxidizing signals for chloroplast redox balance. The finding that chloroplast enzyme oxidation in the dark is delayed in mutants lacking 2-Cys PRXs [32,41–43] confirmed the participation of these enzymes in this rapid oxidative process. Further studies have demonstrated the key role of chloroplast 2-Cys PRX-dependent oxidative signaling in fine-tuning photosynthetic carbon assimilation [44].

The important contribution of oxidizing signals mediated by 2-Cys PRXs to photosynthetic performance raises the issue of the participation in this process of the other thiol peroxidases present in chloroplasts. Based on the finding that Arabidopsis mutants combining the lack of 2-Cys PRXs with those of PRX IIE or PRX Q display similar rates of stromal enzymes oxidation in the dark than the mutant devoid of 2-Cys PRXs [41], it was ruled out a significant role for these atypical PRXs in this oxidative process. Additional candidates to participate in the oxidative component of chloroplast redox regulation are GPX1 and GPX7 since both enzymes display TRX-dependent peroxidase activity. However, the participation of GPXs in chloroplast redox balance or their functional relationship with the NTRC-2-Cys PRX redox system have been scarcely analyzed. In this work, we have addressed these issues by a combination of genetic, physiological, and biochemical approaches. The functional relationship of chloroplast GPXs and 2-Cys PRXs was analyzed by generating the Arabidopsis *2cpab-gpx1gpx7* quadruple mutant, which is simultaneously devoid of chloroplast 2-Cys PRXs and GPXs 1 and 7, whereas the relationship of chloroplast GPXs and NTRC was addressed by generating the *ntrc-gpx1gpx7* mutant. Our results allow to establish the hierarchy of thiol-dependent peroxidases in the chloroplast redox network and their impact on photosynthetic performance and plant growth.

2. Materials and methods

2.1. Biological material and growth conditions

Arabidopsis thaliana (Ecotype Columbia) wild type (WT) and mutant plants were grown on soil in culture chambers under long-day (16 h light/8 h darkness) or short-day (8 h light/16 h darkness) photoperiods at 22 °C and 20 °C during the day and night periods, respectively, at light intensity of 120 μE m^{-2} s^{-1} and 70% relative humidity. For high light (HL) treatments, plants grown under short-day photoperiod for 6 weeks were exposed at a light intensity of 800 μE m^{-2} s^{-1} for the time indicated in the figure legend. *Escherichia coli* strains were grown in liquid Miller nutrient at 37 °C with the appropriate antibiotics.

2.2. Generation of Arabidopsis double, triple and quadruple mutans

To generate the *gpx1gpx7* double mutant, single mutants *gpx1* (SALK_027373) and *gpx7* (SALK_072007), obtained from the European Arabidopsis Stock Centre (Nottingham University, UK), were manually crossed and the *gpx1gpx7* double mutant was selected from the progeny by analyzing the T-DNA insertion in genomic DNA using the oligonucleotides shown in Table S1. The *2cpab-gpx1gpx7* quadruple mutant and the *ntrc-gpx1gpx7* triple mutant were generated by manually crossing the above described *gpx1gpx7* mutant with the *2cpab* [41] and the *ntrc* mutant [45], respectively. The *2cpab-gpx1gpx7* and *ntrc-gpx1gpx7* were selected from the progeny of these crosses by analyzing the presence of the T-DNA insertions in genomic DNA with oligonucleotides indicated in Table S1.

2.3. Protein extraction, alkylation assays and Western blot analysis

Leaves tissues were dissected and immediately frozen with liquid nitrogen. Protein extracts were prepared with extraction buffer (50 mM Tris-HCl, pH 8.0, 0.15 M NaCl, 0.5% (v/v) Nonidet P-40), which was immediately added to leaves tissues that were ground under liquid nitrogen. After mixing on a vortex, extracts were centrifuged at 16,100 *g* at 4 °C for 20 min. Protein was quantified using the Bradford reagent (Bio-Rad). Alkylation assays were performed as reported previously [46] using 60 mM iodoacetamide. Protein samples were subjected to SDS-PAGE under reducing or non-reducing conditions, as indicated in the corresponding figure legends, using acrylamide gel concentration of 9.5% for Rubisco activase (RCA) and γATPase, or 12% for NTRC, 2-Cys PRXs and GPXs, unless otherwise specified. Separated proteins were transferred to nitrocellulose membranes and probed with the indicated antibody. Specific antibodies for NTRC [45] and 2-Cys PRXs [38] were previously raised in our laboratory. The anti-RCA antibody was kindly provided by Dr. A. R. Portis (USDA, Urbana, USA), and the γATPase and GPX antibodies were purchased from Agrisera (Sweden).

2.4. Determination of chlorophylls, measurements of chlorophyll *a* fluorescence and determination of carbon assimilation rates

Chlorophyll was measured as previously described [38]. Room temperature chlorophyll *a* fluorescence of PSII was measured using the pulse-amplitude modulation fluorometers DUAL-PAM-100 (Walz) and IMAGING-PAM M-Series (Walz), as indicated in the figure legends. For DUAL-PAM-100 determinations, induction-recovery curves were performed using red (635 nm) actinic light at 100 μE m^{-2} s^{-1} for 6 min. Saturating pulses of red light at 10000 μE m^{-2} s^{-1} intensity and 0.6 s duration were applied every 60 s and recovery in darkness was recorded for up to 3 min. For IMAGING-PAM M-Series determinations, induction-recovery curves were performed using actinic light at 81 μE m^{-2} s^{-1} for 7 min. Saturating pulses of red light at 10000 μE m^{-2} s^{-1} intensity and 0.6 s duration were applied every 40 s and recovery in darkness was recorded for up to 8 min. The parameters Y(II) and Y (NPQ), corresponding to the quantum yields of PSII photochemistry and non-photochemical quenching, respectively, were calculated according to reported equations [47]. The maximum quantum yield of PSII was determined, using the IMAGING-PAM M-Series, after incubation of plants in the dark for 30 min by calculating the ratio of the variable fluorescence, F_v, to maximal fluorescence, F_m (F_v/F_m). Net CO_2 assimilation rate (A_N) was measured using an open gas exchange system

Li-6400 equipped with the chamber head (Li-6400–40) in dark-adapted leaves of plants that had been grown under long-day for four weeks, and were carried out by the Service for Photosynthesis, Instituto de Recursos Naturales y Agrobiología de Sevilla (Spain).

2.5. Cloning, expression, and purification of recombinant proteins

For the expression of Arabidopsis GPX1 and GPX7, the corresponding cDNAs, excluding the predicted transit peptides and the stop codons, were amplified with iProof™ High-Fidelity DNA Polymerase (Bio-Rad) using oligonucleotides listed in Table S1, which added *Nco*I and *Xho*I sites at the 5' and 3' ends, respectively. For the expression of Arabidopsis TRX *m*4, the corresponding cDNA, excluding the predicted transit peptides and including the stop codon, was amplified as described above using oligonucleotides (Table S1) adding *Bam*HI and *Hind*III sites at the 5' and 3' ends, respectively. PCR products were gel-purified, cloned in pGEMt vector (Promega), and sequenced. For GPXs, pGEMt-derived plasmids were digested with *Nco*I and *Xho*I, subcloned in the pET28 (Qiagen) expression vector and introduced into *E. coli* BL21 (DE3) cells. The pGEMt-TRX *m*4 plasmid was digested with *Bam*HI and *Hind*III, subcloned in the pQE30 (Qiagen) expression vector and introduced into *E. coli* XL1Blue. Over-expressed recombinant proteins, containing a His-tag at the C-terminus (GPX1 and GPX7) or the N-terminus (TRX *m*4), were purified by nitrile triacetic acid (NTA) affinity chromatography in Hi-Trap affinity columns (GE Healthcare). Recombinant His-tagged NTRC and 2-Cys PRX from rice [38] and TRXs of the types *y*2, *x* and *f2* from Arabidopsis were obtained as previously described [31,41].

2.6. In vitro redox state determinations and activity assays

The ability of NTRC to reduce GPXs was tested as the oxidation of NADPH following the absorbance at 340 nm [38] in reaction mixtures containing 100 mM phosphate buffer, pH 7.2, 2 mM EDTA, 0.25 mM NADPH, 0.5 mM hydrogen peroxide and the referred enzymes NTRC and GPXs at final concentrations of 2 μM and 6 μM, respectively. For monitoring the reduced and oxidized forms of peroxidases, recombinant 2-Cys PRX, GPX1 and GPX7, at a final concentration of 6 μM, were incubated for 30 min in 50 mM phosphate buffer, pH 7.4, in the presence or absence of 30 mM dithiothreitol (DTT), as source of reducing power. To test the ability of NTRC to reduce GPXs in shift assays, the reaction mixture included NADPH (0.25 mM) instead of DTT. Proteins were separated by non-reducing SDS-PAGE using a 14% acrylamide gel and

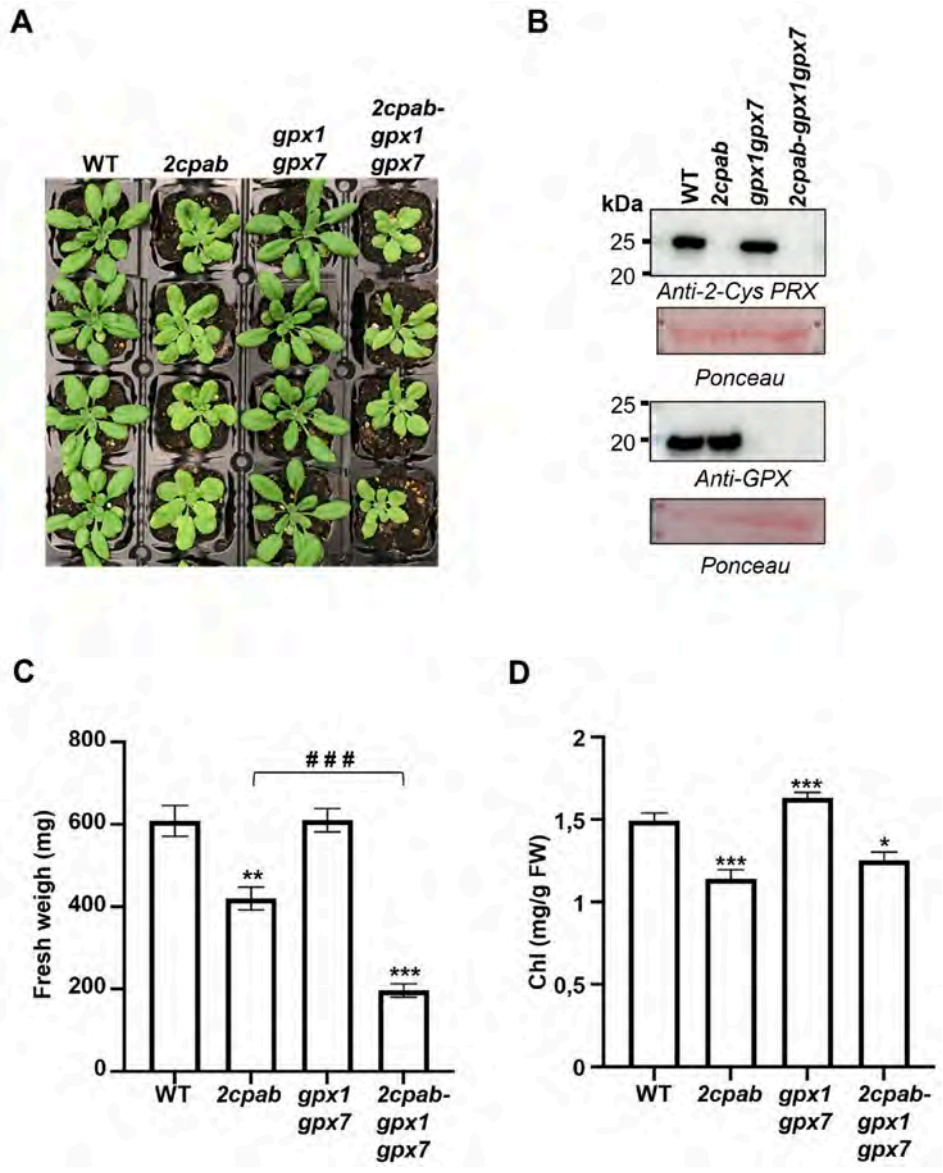

Fig. 1. Growth phenotypes of Arabidopsis mutants simultaneously devoid of GPX1, GPX7 and 2-Cys PRXs. (A) Wild type and *2cpab*, *gpx1gpx7* and *2cpab-gpx1gpx7* mutant plants, as indicated, were grown under long-day photoperiod for 4 weeks. **(B)** Western blot analysis of the levels of 2-Cys PRXs and chloroplast GPXs, 1 and 7. Protein extracts were obtained from rosette leaves of plants grown as in (A) and subjected to SDS-PAGE under reducing conditions, transferred to nitrocellulose filters and probed with anti-2-Cys PRX or anti-GPX antibodies. Molecular mass markers (kDa) are shown on the left and even loading is indicated by Ponceau staining of the Rubisco large subunit. The weight of the rosettes **(C)** and chlorophyll levels **(D)** were determined from at least 8 plants grown as in (A) and represented as average values ± SEM. Asterisks represent significant differences compared with the wild type (*, $P < 0.05$; **, $P < 0.01$; ***, $P < 0.001$, Student's *t*-test). Hashes indicate significant differences between *2cpab* and *2cpab-gpx1gpx7* ($^{###}$, $P < 0.001$, Student's *t*-test).

stained with Coomassie blue. Redox interaction between GPXs and TRXs was monitored in reaction mixtures containing hydrogen peroxide (0.5 mM), DTT (0.1 mM) and the indicated GPX and TRX isoforms at concentrations of 2 μM and 10 μM, respectively. Reactions were incubated for 15 min at room temperature and measured spectrophotometrically at 560 nm. The consumption of hydrogen peroxide was determined as previously described [41], using the ferrous ion oxidation (FOX) assay in the presence of xylenol orange.

3. Results

3.1. The lack of chloroplast GPXs aggravates the growth inhibition phenotype caused by the lack of 2-Cys PRXs

With the aim of analyzing the function of GPXs in chloroplast redox homeostasis, an Arabidopsis *gpx1gpx7* double mutant was generated by manually crossing individual Arabidopsis T-DNA mutants *gpx1* and *gpx7*. Western blot analysis confirmed the absence of chloroplast GPX1 and GPX7 in the *gpx1gpx7* double mutant (Fig. 1A and B), which displayed a growth phenotype indistinguishable of the WT when grown under long-day photoperiod (Fig. 1A), as shown by the fresh weight of rosette leaves (Fig. 1C), and leaf chlorophyll contents (Fig. 1D). Therefore, the lack of chloroplast GPXs has no marked effect on plant growth, at least under the standard conditions used in this work. To analyze the functional interaction of chloroplast GPXs and 2-Cys PRXs, we took advantage of the previously reported *2cpab* double mutant [41], which is a double knockout lacking 2-Cys PRXs A and B, as confirmed by Western blot analysis (Fig. 1B). After manually crossing the *2cpab* and *gpx1gpx7* mutants, the *2cpab-gpx1gpx7* quadruple mutant was selected. Western blot analysis confirmed the absence of chloroplast 2-Cys PRXs and GPXs in the quadruple mutant (Fig. 1B). Though the leaf chlorophyll content was similar in the *2cpab* and *2cpab-gpx1gpx7* mutants (Fig. 1D), the lack of GPXs 1 and 7 in the *2cpab* background resulted in a more severe growth inhibition than that of the *2cpab* mutant, as revealed by the lower rosette leaves fresh weight of the quadruple mutant (Fig. 1C). Thus, the lack of GPX1 and GPX7, which has no significant effect on plant growth in the WT background, does affect growth of plants simultaneously devoid of chloroplast 2-Cys PRXs.

To further test the functional relationship of chloroplast GPXs and 2-Cys PRXs, different photosynthetic parameters in the lines under analysis were determined. In dark-adapted plants the quantum yield of PSII [Y(II)] values in the WT were very similar to those observed in *gpx1gpx7* and 2-Cys Prxs depleted mutants (Fig. 2A). Immediately after illumination, the WT showed the expected drop to minimal Y(II) values, which was like that observed in the *gpx1gpx7* mutant (Fig. 2A, inset). In agreement with previous results [41], the *2cpab* mutant displayed a lower drop of Y(II), which was even lower in the *2cpab-gpx1gpx7* mutant (Fig. 2A, inset). These results indicate decreased level of reduction of the PQ pool probably related to a more rapid activation of photosynthetic metabolism in plants simultaneously devoid of chloroplast 2-Cys PRXs and GPXs than in the WT and the *gpx1gpx7* double mutant, as shown by the higher Y(II) values in the *2cpab* and *2cpab-gpx1gpx7* mutants during the following light period (Fig. 2A). The lack of chloroplast GPXs also affected the quantum yield of Non-Photochemical Quenching [Y(NPQ)], which was slightly higher in the *gpx1gpx7* mutant than in the WT, and in the *2cpab-gpx1gpx7* than in the *2cpab* mutant (Fig. 2B), thus indicating a slight effect of chloroplast GPXs on heat dissipation, which was observed in both, WT and *2cpab* backgrounds. Regarding the rate of CO_2 fixation (A_N), the *gpx1gpx7* mutant displayed values comparable to those of the WT, whereas the *2cpab-gpx1gpx7* and *2cpab* mutants showed similar but slightly lower rates (Fig. 2D). Altogether, these results indicate that the lack of chloroplast GPXs affects growth only in plants devoid of 2-Cys PRXs, which show slightly altered PSII performance.

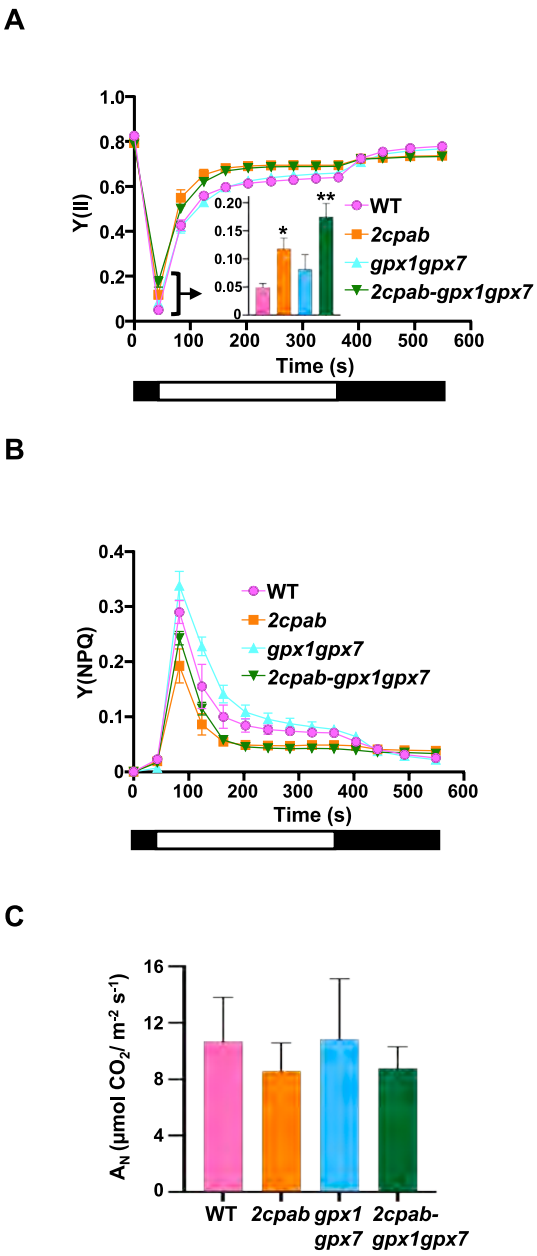

Fig. 2. Comparative analysis of the photosynthetic performance of mutants devoid of chloroplast GPXs and 2-Cys PRXs. Measurements of quantum yields of photosystem II photochemistry [Y(II)] **(A)** and non-photochemical quenching [Y(NPQ)] **(B)** were performed using a DUAL-PAM-100 fluorometer, in plants of the indicated genotypes, grown under long-day conditions for 4 weeks. Values are the average of three determinations and standard errors of the mean (SEM) are represented as error bars. White and black blocks indicate periods of illumination with actinic light (81 μE m^{-2} s^{-1}) and darkness, respectively. Inset in (A) shows Y(II) values immediately after illumination. Asterisks represent significant differences compared with the wild type (*, $P < 0.05$; **, $P < 0.01$, Student's *t*-test). No significant differences were found between *2cpab* and *2cpab-gpx1gpx7*. **(C)** Net CO_2 assimilation rate (A_N) was measured using an open gas exchange system in dark-adapted leaves from three plants. Mean ± SD are represented.

3.2. GPXs and 2-Cys PRXs act concertedly on chloroplast enzyme oxidation in the dark

Once analyzed the effect of GPXs 1 and 7 on plant growth and photosynthetic performance, we sought to analyze their functional relationship with 2-Cys PRXs in the redox regulation of chloroplast

enzymes in response to light and darkness. To that end, we focused on Rubisco activase (RCA) and the γ subunit of ATPase (γATPase), which are well-established redox regulated enzymes. As expected, both proteins were fully oxidized in dark-adapted plants (Fig. 3A, C). After 30 min under growth light intensity (120 μE m^{-2} s^{-1}), RCA was slightly more reduced in the *gpx1gpx7* mutant than in the WT, though it was not statistically significant (Fig. 3A and B). The level of light-dependent reduction of RCA was higher in the *2cpab* mutant, as expected, but was not further increased in the *2cpab-gpx1gpx7* mutant (Fig. 3A and B). In contrast, γATPase was fully reduced in all the lines analyzed (Fig. 3C and D), in agreement with the high sensitivity of this protein to light-dependent reduction. Therefore, GPXs have a minor contribution, if any, to the role of 2-Cys PRXs in the control of the redox state of chloroplast enzymes in the light. We then analyzed the participation of GPXs in the oxidation of these enzymes in the dark. With that purpose, dark-adapted plants were incubated for 30 min under high light intensity (800 μE m^{-2} s^{-1}), which caused complete reduction of RCA (Fig. 4A and B) and almost full reduction of γATPase (Fig. 4C and D), and subsequently transferred to darkness to determine the rate of protein oxidation. RCA oxidation was slightly delayed in the *gpx1gpx7* mutant, as compared with the WT, whereas the *2cpab* mutant showed the expected higher delay in enzyme oxidation, which was further aggravated in the *2cpab-gpx1gpx7* mutant (Fig. 4A and B). The rate of γATPase oxidation in the dark followed a similar pattern, oxidation being almost not affected in the *gpx1gpx7* mutant, as compared with the WT, whereas the *2cpab-gpx1gpx7* mutant showed a higher delay of γATPase oxidation than the *2cpab* mutant (Fig. 4C and D). Thus, the analyses of the redox state of RCA and γATPase indicate a more relevant role of chloroplast GPXs in dark-dependent enzyme oxidation than in light-dependent enzyme reduction.

3.3. The activity of chloroplast GPXs is independent of NTRC

The finding that decreased contents of 2-Cys PRXs suppress the severe growth inhibition phenotype of the *ntrc* mutant [40] revealed the tight functional relationship of NTRC and 2-Cys PRXs in maintaining the redox balance of chloroplasts. Thus, to further explore the contribution of GPX1 and GPX7 to chloroplast redox homeostasis, we sought to analyze their genetic interaction with NTRC. With that purpose, the *gpx1gpx7* double mutant was manually crossed with the *ntrc* mutant and the *ntrc-gpx1gpx7* triple mutant was selected. Western blot analysis confirmed the lack of NTRC and GPXs 1 and 7 in the triple mutant (Fig. 5A and B), however, the lack of these GPXs in the *ntrc* background did not have any suppressor nor aggravated effect on the growth phenotype of the *ntrc* mutant as shown by the fresh weight (Fig. 5A, C) and chlorophyll contents (Fig. 5A, D) of the rosette leaves. In line with their similar growth rates, the *ntrc* and *ntrc-gpx1gpx7* mutants also showed almost indistinguishable values of Y(II) (Fig. S1A) and Y(NPQ) (Fig. S1B), as well as the rate of CO_2 fixation (Fig. S1C). The similarity of the *ntrc* and *ntrc-gpx1gpx7* mutants was further confirmed by analyzing the redox state of RCA in response to light and darkness. Both mutants showed severely impaired light-dependent reduction of RCA (Figs. S2A and B), whereas the expected accelerated oxidation of RCA in the dark in the *ntrc* mutant was only slightly increased in the *ntrc-gpx1gpx7* mutant (Figs. S2C and D). Therefore, the comparative analysis of the *ntrc* and *ntrc-gpx1gpx7* mutants suggests that the participation of chloroplast

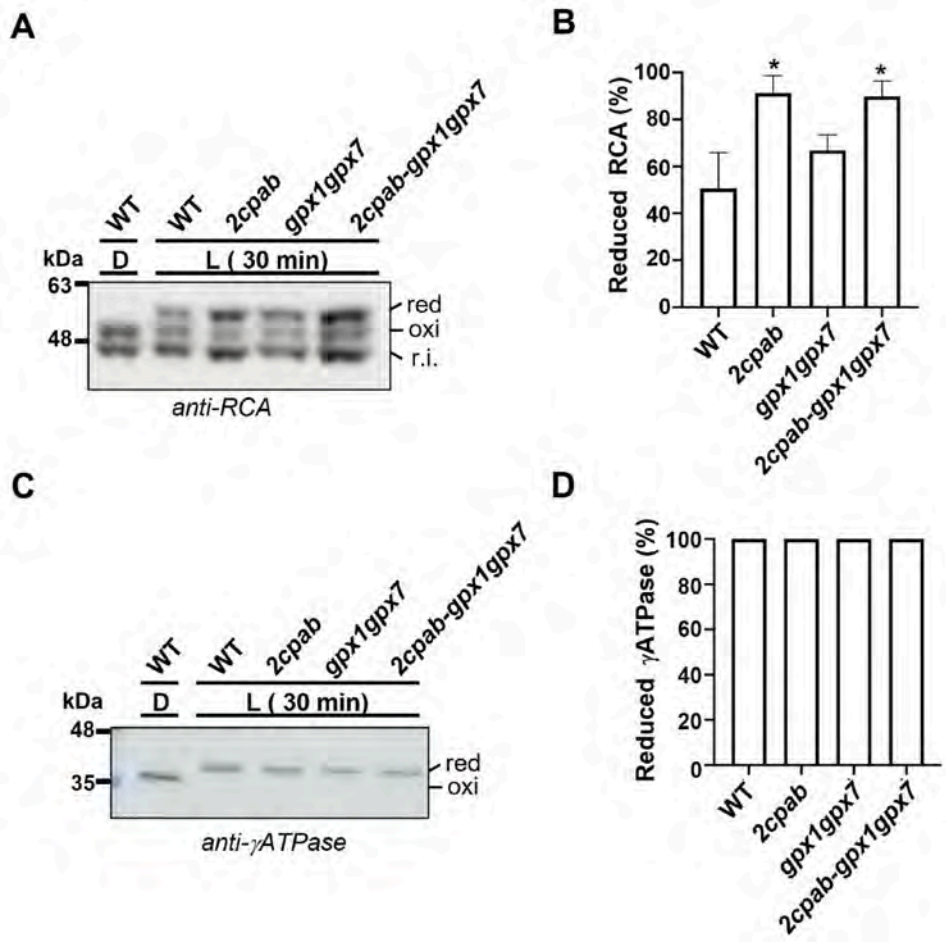

Fig. 3. Effect of the lack of GPXs and 2-Cys PRXs on the light-dependent reduction of RCA and γATPase. Wild type and mutant plants were grown under long-day conditions for 4 weeks at a light intensity of 120 μE m^{-2} s^{-1}. The *in vivo* redox state of RCA **(A)** and γATPase **(C)** were determined at the end of the dark period (D), and after 30 min of illumination at 120 μE m^{-2} s^{-1} (L) by labelling of the thiol groups with the alkylating agent iodoacetamide. Molecular mass markers (kDa) are indicated on the left. Band intensities were quantified (Gel Analyzer) and the percentage of reduction, determined as the ratio between the reduced form and the sum of reduced and oxidized forms, of RCA **(B)** and γATPase **(D)** is represented as the mean ± SEM of three independent experiments. Statistical significance compared with the wild type is indicated (*, $P < 0.05$, Student's *t*-test). No significant differences were found between *2cpab* and *2cpab-gpx1gpx7*. red, reduced; oxi, oxidized; r.i., redox insensitive.

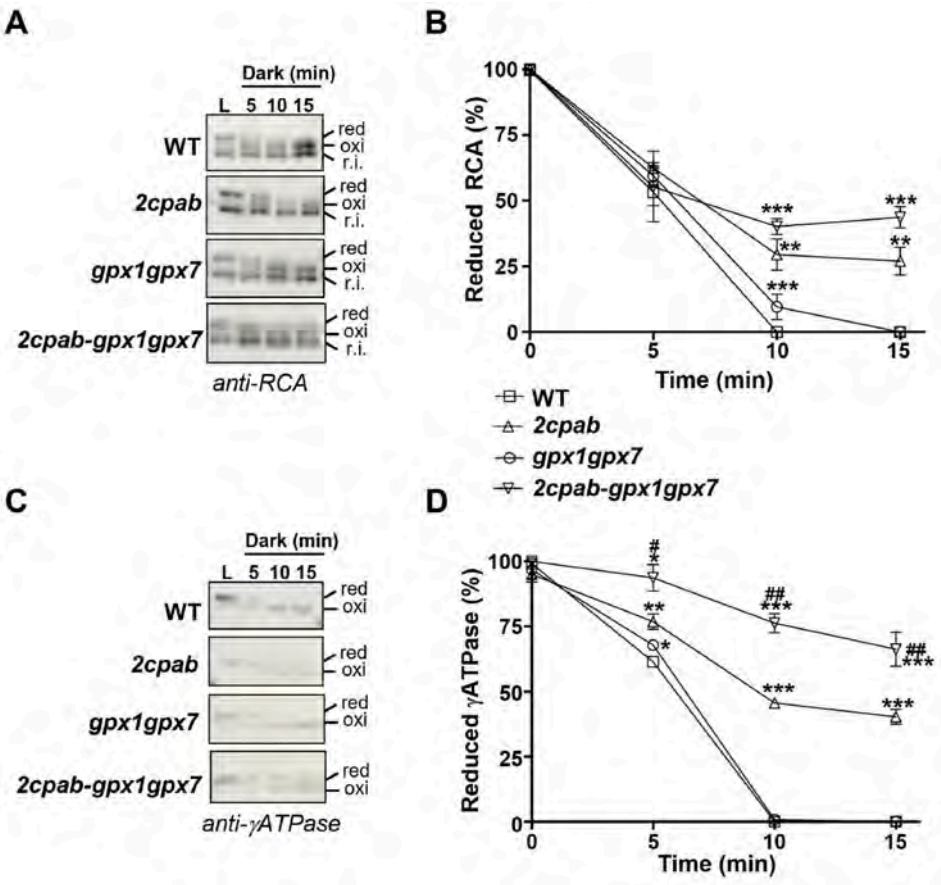

Fig. 4. Effect of the lack of GPXs and 2-Cys PRXs on the dark-dependent oxidation of RCA and γATPase. Wild type and mutant plants were grown under long-day conditions for 4 weeks at a light intensity of 120 μE m^{-2} s^{-1}. At the end of the night period, plants were exposed to a light intensity of 800 μE m^{-2} s^{-1} during 30 min (L), then light was switched off and samples were harvested at 5, 10 and 15 min. The *in vivo* redox state of RCA **(A)** and γATPase **(C)** at the indicated times was determined by labelling of the thiol groups with the alkylating agent iodoacetamide. Band intensities were quantified (Gel Analyzer) and the percentage of reduction of RCA **(B)** and γATPase **(D)**, determined as the ratio between the reduced form and the sum of reduced and oxidized forms, is represented as the mean ± SEM of three independent experiments. Statistical significance compared with the wild type is indicated (*, $P < 0.05$; **, $P < 0.01$; ***, $P < 0.001$, Student's *t*-test). Hashes indicate significant differences between *2cpab* and *2cpab-gpx1gpx7* ($^{\#}$, $P < 0.05$; $^{\#\#}$, $P < 0.01$, Student's *t*-test). red, reduced; oxi, oxidized; r.i., redox insensitive.

GPXs in the redox balance of the organelle is independent of NTRC.

Finally, the functional relationship of chloroplast GPXs with 2-Cys PRXs and NTRC based on genetic analyses was complemented with biochemical assays. To that end, Arabidopsis GPX1 and GPX7 devoid of their putative transit peptides, were expressed in *E. coli* fused to a His-tag and purified by Hi-Trap chromatography. Both enzymes are redox sensitive as revealed by the different electrophoretic mobility shown in the presence or absence of DTT (Fig. S3). To analyze the interaction of GPX1 and GPX7 with chloroplast TRXs, a similar approach was used to express in *E. coli* His-tagged representatives of Arabidopsis typical TRXs (TRX *f*2, TRX *m*4, TRX *x*, and TRX *y*2). For comparison, the well-established interaction of 2-Cys PRX and NTRC from rice was used as positive control. As previously reported [38], the incubation of NTRC and 2-Cys PRX in the presence of NADPH and hydrogen peroxide resulted in the rapid oxidation of NADPH (Fig. 6A) and the reduction of most of the 2-Cys PRX present in the reaction mixture after 10 min of incubation, as indicated by the conversion of the dimeric (oxidized) into the monomeric (reduced) form of the enzyme (Fig. 6B). Conversely, neither oxidation of NADPH (Fig. 6A) nor reduction of GPX1 and GPX7 (Fig. 6B) were observed when 2-Cys PRX was replaced by GPX1 or GPX7, confirming the inability of NTRC to reduce chloroplast GPXs. To identify the electron donor of chloroplast GPXs, the peroxidase activity of these enzymes was assayed in the presence of representative chloroplast TRXs. Fig. 6C shows that TRX *y*2 is the most efficient electron donor for the peroxidase activity of GPX1 and GPX7. Though with much lower efficiency, GPX1 and GPX7 were also reduced by TRX *m*4 and TRX *f*2, whereas TRX *x* showed almost negligible activity (Fig. 6C).

3.4. The simultaneous lack of chloroplast 2-Cys PRXs and GPXs has minor effects on plant response to high light

Previous reports had proposed an antioxidant function for TRXs *y* and *x* based on the ability of these TRXs to reduce 2-Cys PRXs [29–31]. Thus, the finding that TRX *y*2 is the most efficient reductant of chloroplast GPXs prompted us to test the sensitivity of the mutants under analysis to treatments that cause oxidative stress such as HL. Plants that had been grown under short-day photoperiod (light intensity during the day periods of 120 μE m^{-2} s^{-1}) for 6 weeks were incubated for up to 12 h under HL (800 μE m^{-2} s^{-1}) and the effect of this treatment on PSII stability was tested by analyzing the F_v/F_m ratio. Before starting the HL treatment (Fig. 7, 0 h), the *2cpab* mutant showed slightly lower level of F_v/F_m than the WT, as previously reported [46], confirming the effect of the lack of 2-Cys PRXs on PSII stability. The F_v/F_m ratio of the *gpx1gpx7* mutant was like that of the WT, whereas the *2cpab-gpx1gpx7* and *2cpab* mutants showed similar F_v/F_m ratios (Fig. 7), indicating the lack of effect of chloroplast GPXs on PSII stability under standard growth conditions, in agreement with above mentioned results (Fig. 2A–D). The HL treatment provoked the decline of the F_v/F_m ratio after 6–12 h, however, the effect was similar in the *gpx1gpx7* mutant and the WT (Fig. 7). The most negative effect of HL was observed in the *2cpab-gpx1gpx7* mutant after 12 h of treatment (Fig. 7).

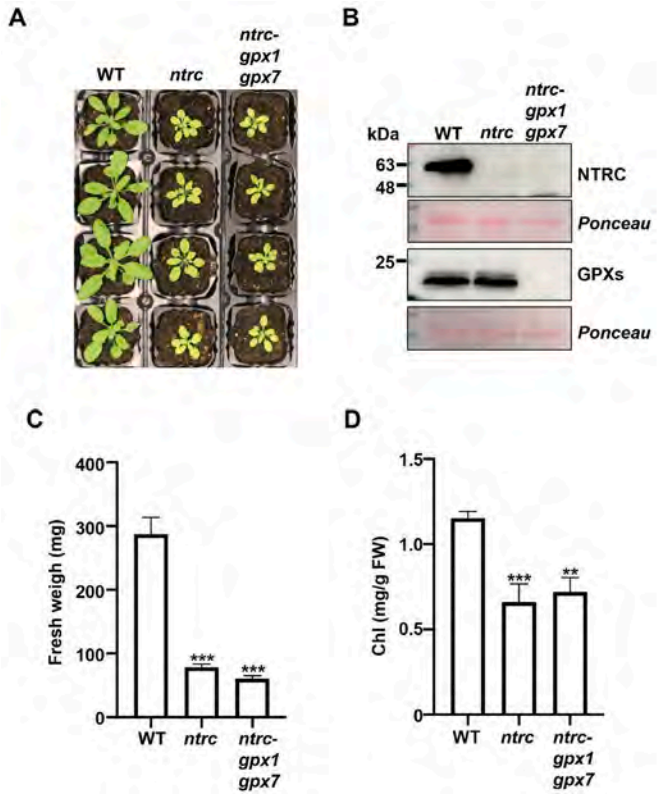

Fig. 5. Growth phenotypes of Arabidopsis mutants simultaneously devoid of GPX1, GPX7 and NTRC. (A) Wild type and mutant plants, as indicated, were grown under long-day photoperiod for 4 weeks. **(B)** Western blot analysis of the levels of NTRC and GPXs, 1 and 7. Protein extracts were obtained from rosette leaves of plants grown as in (A) and subjected to SDS-PAGE under reducing conditions, transferred to nitrocellulose filters and probed with anti-NTRC or anti-GPX antibodies. Even loading was monitored by Ponceau staining of the Rubisco large subunit. Molecular mass markers (kDa) are indicated on the left. The weight of the rosettes **(C)** and chlorophyll levels **(D)** were determined from at least 8 plants grown as in (A) and represented as average values ± SEM. Asterisks represent significant differences compared with the wild type (**, $P < 0.01$; ***, $P < 0.001$, Student's *t*-test). No significant differences were found between *ntrc* and *ntrc-gpx1gpx7*.

4. Discussion

4.1. Chloroplast GPXs are dispensable for plant growth under standard conditions

The aim of this work was to determine the contribution of chloroplast-localized GPXs to the redox homeostasis of the organelle and establish their functional interaction with the NTRC-2-Cys PRXs redox system. Previous analyses of single mutants of Arabidopsis lacking individual GPXs showed no alteration of their shoot phenotype [48], however, the Arabidopsis chloroplast contains two GPXs [20,49], which might have redundant functions. Thus, as a first approach to address the participation of GPXs on photosynthetic performance and plant growth the *gpx1gpx7* double mutant, which lacks the two chloroplast-localized GPXs of Arabidopsis (Fig. 1A and B), was generated. The growth phenotype of the *gpx1gpx7* mutant, which was indistinguishable of the WT (Fig. 1A, C, D), indicates that these GPXs are dispensable for plant growth. In line with the WT-like growth phenotype of the *gpx1gpx7* mutant, the analysis of the photochemical parameters revealed only minor effects of the lack of chloroplast GPXs on PSII performance as shown by the slightly higher levels of Y(NPQ) of the *gpx1gpx7* mutant, as compared with the WT (Fig. 2B), and the drop of Y(II) immediately after illumination of dark-adapted plants, which was slightly lower in the *gpx1gpx7* mutant than in the WT (Fig. 2A, inset), though it was indistinguishable from the WT in the following light and dark periods (Fig. 2A). Despite this minor effect on PSII, which might be exerted by affecting proteins such as High Chlorophyll Fluorescent 244 (HCF244), a protein involved in PSII biogenesis which has been shown to interact with GPX7 [50], no alterations were observed on the CO_2 fixation rate (Fig. 2C), further supporting the WT-like growth phenotype of the *gpx1gpx7* mutant under standard conditions (Fig. 1A–D).

An additional possibility is that chloroplast GPXs are relevant for plant response to environmental stresses as suggested by studies of GPXs expression in response to abiotic stresses [11,20]. In this regard, it was reported that depletion of chloroplast GPXs in Arabidopsis compromised photooxidative stress tolerance [51], however, Arabidopsis mutants devoid of individual GPXs did not show drastic changes in response to salt and osmotic stresses [52], suggesting a minor role of these enzymes in plant response to stress. In line with this notion, the *gpx1gpx7* mutant behaved like the WT in response to HL (Fig. 7). Nevertheless, after 12 h of HL treatment, the *2cpab-gpx1gpx7* mutant was more affected than the *2cpab* mutant (Fig. 7), thereby suggesting that the concerted action of GPXs and 2-Cys PRXs is needed for plant response to photooxidative stress.

4.2. The simultaneous lack of chloroplast GPXs and 2-Cys PRXs affects the redox balance of the organelle and plant growth

The contribution of GPX1 and GPX7 to the complex redox network of chloroplasts was addressed by analyzing their functional relationship with the NTRC-2-Cys PRXs redox system. Chloroplast metabolism is tightly linked to light fluctuations through ferredoxin (FDX), the final acceptor of the photosynthetic electron transport chain, which delivers reducing equivalents to TRXs via FDX-dependent TRX reductase (FTR) thereby allowing the reduction, and activation, of key redox-regulated enzymes of biosynthetic metabolic pathways, such as the Calvin-Benson cycle [53–56]. Besides this reductive pathway, the finding that atypical chloroplast TRXs such as ACHT1 [34], ACHT4 [35] and TRX L2 [32] display oxidizing activity mediated by 2-Cys PRXs uncovered the essential contribution of oxidizing signals for fine-tuning the redox balance of the organelle in response to changes in light intensity and darkness [44]. These results raised the question of the role of GPXs in chloroplast redox homeostasis since the peroxidase activity of these enzymes is supported by TRXs hence being very similar to the peroxidase activity of 2-Cys PRXs [11,21,22]. The aggravated growth inhibition of the *2cpab-gpx1gpx7*, as compared with the *2cpab* mutant (Fig. 1A, C), indicates the concerted action of both thiol-peroxidases on plant growth. In agreement with previous results [41,42], the *2cpab* mutant showed a lower drop of Y(II) immediately after illumination than the WT and this effect was increased in the *2cpab-gpx1gpx7* mutant (Fig. 2A, inset). Furthermore, the *2cpab-gpx1gpx7* mutant showed higher levels of NPQ than the *2cpab* mutant (Fig. 2B), whereas no additional effects of the simultaneous lack of GPXs and 2-Cys PRXs were observed on CO_2 fixation rates (Fig. 2C). Moreover, the drop of Y(II) immediately after illumination reflects the full reduction of the PQ pool while biosynthetic metabolism is activated. While these results show the concerted contribution of GPXs and 2-Cys PRXs to chloroplast redox homeostasis, it is not clear that these effects are sufficient to explain the growth inhibition phenotype of the *2cpab-gpx1gpx7* mutant, thus further studies will be needed to identify additional processes affected by chloroplast GPXs.

4.3. The effect of GPXs on chloroplast redox balance is independent of NTRC

The suppressor effect of the *ntrc* phenotype by decreased contents of 2-Cys PRXs [40] uncovered the tight functional relationship of NTRC and 2-Cys PRXs in maintaining chloroplast redox balance. Thus, to establish the role of GPXs in chloroplast redox homeostasis, a key

question is the functional relationship of these thiol-peroxidases and NTRC, which was addressed in this work by a combination of genetic and biochemical approaches. Unlike the *ntrc-Δ2cp* [40] and the *ntrc-2cpab* [46] mutants, which show the suppressor effect of the *ntrc* phenotype by the deficiency of 2-Cys PRXs, the triple *ntrc-gpx1gpx7* mutant simultaneously lacking NTRC and chloroplast GPXs (Fig. 5A and B) shows a growth phenotype like the *ntrc* mutant (Fig. 5A, C, D). Moreover, these mutants showed no significant differences of photosynthesis performance, as indicated by the quantum yields of PSII, NPQ and rates of CO_2 fixation (Figs. S1A–C). Similarly, the *ntrc-gpx1gpx7* mutant showed levels of light-dependent RCA reduction (Figs. S2A and B) and dark-dependent RCA oxidation (Figs. S2C and D) like those of the *ntrc* mutant. Altogether, these results strongly support the notion that chloroplast GPXs and NTRC are functionally unrelated. This notion was further supported by *in vitro* assays (Fig. 6A and B) which showed the failure of NTRC to reduce GPXs 1 and 7, whereas in agreement with previous results [45], NTRC showed high activity with 2-Cys PRX. Moreover, assays with recombinant TRXs allowed to establish the preference of Arabidopsis chloroplast GPXs for TRXs *y* (Fig. 6C), as reported for the poplar enzyme [22]. Thus, the effects of the lack of GPXs might be related with the function of TRXs *y*, which is so far poorly understood.

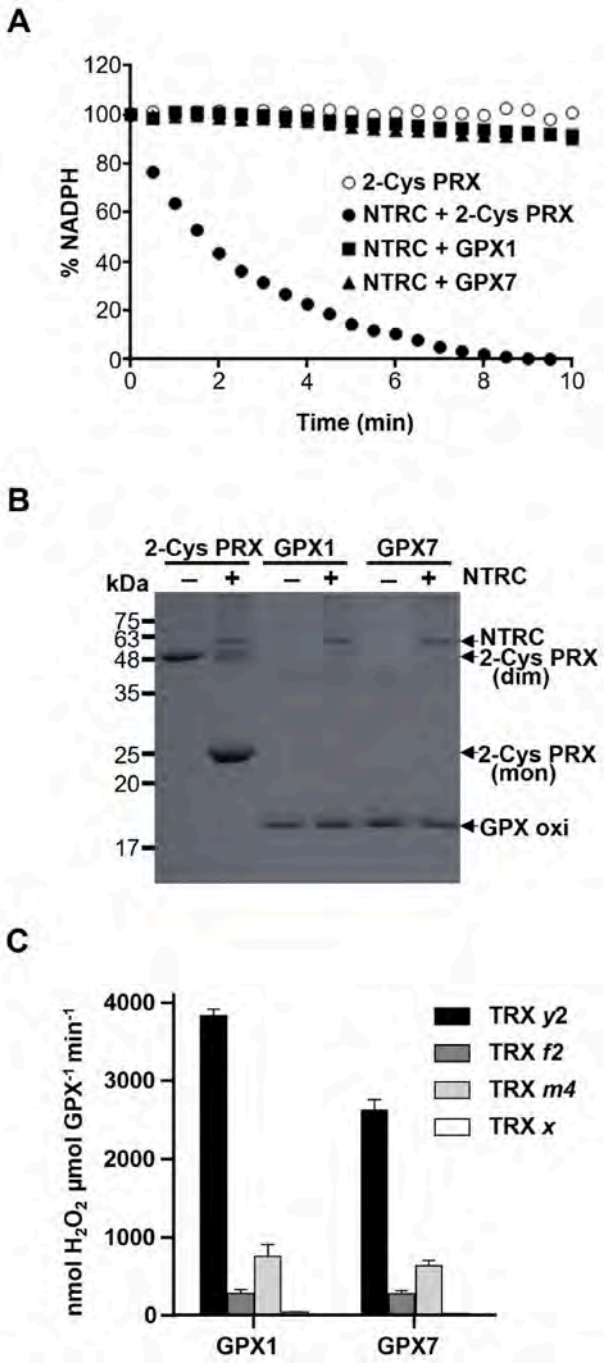

(caption on next column)

Fig. 6. *In vitro* analysis of the interaction of GPX1 and GPX7 with NTRC and TRXs. The redox interaction between GPXs, 1 and 7, and NTRC was monitored by NADPH oxidation **(A)** and mobility shift assays **(B)**. The NADPH oxidation assays **(A)** were performed in reaction mixtures containing 100 mM phosphate buffer, pH 7.0, 2 mM EDTA, 0.25 mM NADPH, 0.5 mM hydrogen peroxide, and the recombinant His-tagged proteins as follows: 2 μM NTRC plus 6 μM GPX1 (closed squares), 2 μM NTRC plus 6 μM GPX7 (closed triangles). Assays containing 2-Cys PRX (6 μM) in the presence (closed circles) or absence (open circles) of NTRC (2 μM) were included as positive and negative controls, respectively. For mobility shift assays **(B)**, GPXs (6 μM) or 2-Cys PRX (6 μM), included here as a positive control, were incubated for 30 min in a reaction mixture containing 100 mM phosphate buffer, pH 7.0, 2 mM EDTA and 0.25 mM NADPH in the presence or absence of NTRC (2 μM), as indicated. Thiols were blocked with iodoacetamide and samples were then subjected to non-reducing SDS-PAGE (14% acrylamide) and stained with Coomassie blue. Reduction of 2-Cys PRX is monitored by the shift from the oxidized dimeric (dim) form to the reduced monomeric (mon) form of the enzyme. Molecular weight markers (kDa) are indicated on the left. **(C)** Redox interaction between GPXs, 1 and 7, and TRXs *y*2, *f*2, *m*4 and *x*, was monitored following the rates of hydrogen peroxide consumption by the ferrous ion oxidation (FOX) assay. Reaction mixtures, containing hydrogen peroxide (0.5 mM), DTT (100 μM) as source of reducing equivalents and the indicated GPX (2 μM) and TRX (10 μM) isoforms, were incubated for 15 min at room temperature and measured spectrophotometrically at 560 nm. Each value is the mean of three independent experiments ± standard error (SEM).

5. Conclusion

In this study, we have used a combination of genetic and biochemical approaches to determine the role of chloroplast GPXs into the complex redox network of the organelle, which is summarized in the scheme shown in Fig. 8. The severe phenotypic consequences of the lack of NTRC [45,57] and 2-Cys PRXs [46,58] support the central role of the NTRC-2-Cys PRXs redox couple in determining the redox state of redox-regulated targets. According to this model (Fig. 8), FDX, the final acceptor of the photosynthetic electron transport chain, delivers reducing equivalents to TRXs, allowing the reduction of redox sensitive targets in response to light, and, via FDX-NADP reductase (FNR) and NADPH, to NTRC. The severe phenotype of Arabidopsis mutants combining the deficiencies of NTRC and TRXs *f* [59,60], and TRX *x* [59], which are suppressed by decreased contents of 2-Cys PRXs [40,61] allows to link the reducing capacity of these TRXs with the NTRC-2-Cys PRXs system (Fig. 8, green pathway). In the light, NTRC maintains the redox balance of 2-Cys PRXs thereby avoiding drainage of electrons from TRXs (Fig. 8, dotted green arrow). This has been shown for typical TRXs of the types *x*, *f*, and *m*, but it is likely that affects other TRXs. In the dark, 2-Cys PRXs mediate the transfer of reducing equivalents to hydrogen peroxide with the participation of oxidizing TRXs such as ACHT1 [34], ACHT4 [35] and TRX L2 [32] (Fig. 8, red pathway), though typical TRXs might also contribute to this oxidative pathway as suggested by *in vitro* assays showing the participation of TRXs *f* and 2-Cys PRX in the oxidation of fructose-1,6-bisphosphatase, among other redox regulated proteins [32,41,42]. Though not analyzed in this work, atypical PRX Q and PRX IIE, as well present in Arabidopsis chloroplasts [15,16], seem to have a minor role in chloroplast redox homeostasis [41]. While PRX Q can be reduced by TRXs *y* [30], PRX IIE was shown to be regenerated by

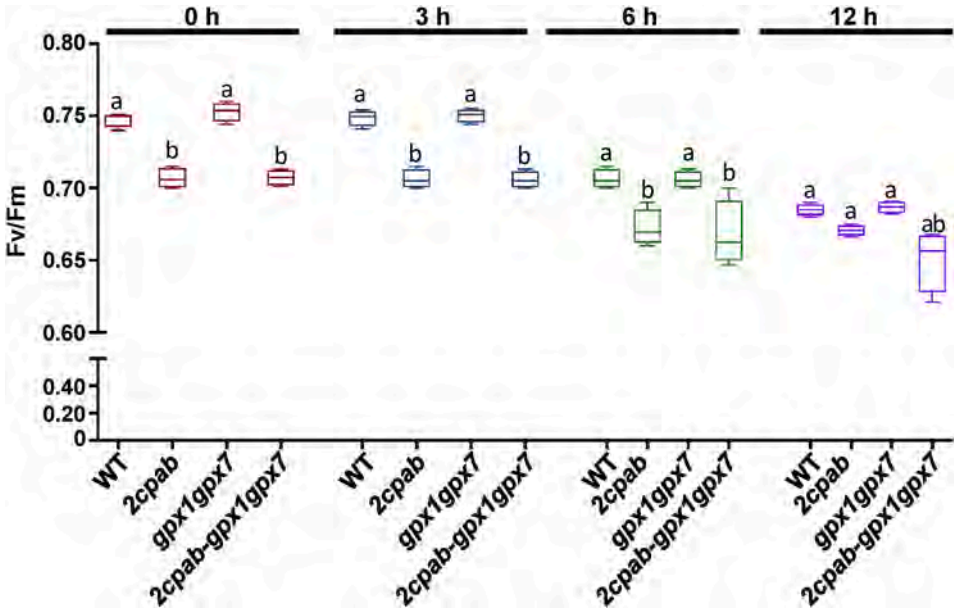

Fig. 7. Effect of short-term high light treatment on wild type and mutant plants devoid of GPX1, GPX7 and/or 2-Cys PRXs. Wild type and mutant plants, as indicated, were grown under short-day photoperiod at a light intensity of 120 μE m^{-2} s^{-1} for 6 weeks and transferred to an intensity of 800 μE m^{-2} s^{-1}. The Fv/Fm, representing the maximum potential quantum efficiency of photosystem II, was measured with an IMAGING-PAM-100 fluorometer before (0 h) and during (3 h, 6 h and 12 h) the high light treatment. Box plots represent mean values ± standard error (SEM) from at least 6 plants. Letters indicate significant differences ($P < 0,05$, one-way Anova) between lines at the indicated time of treatment.

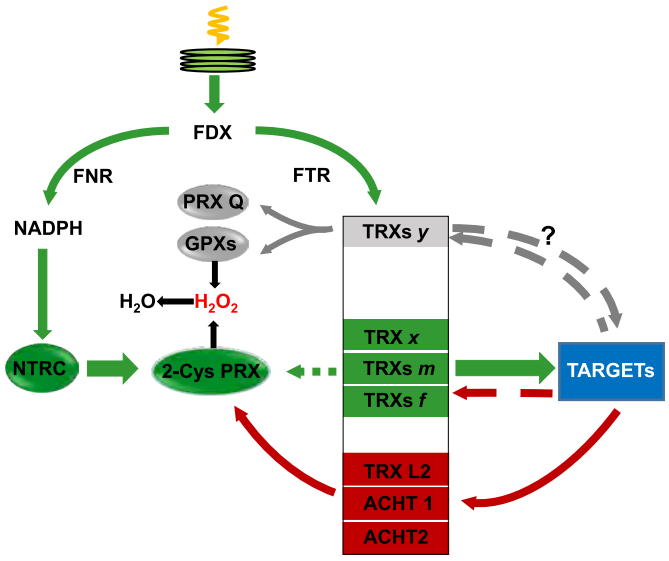

Fig. 8. Proposed model for the contribution of GPXs to the chloroplast redox homeostasis. The photosynthetic electron transport chain delivers reducing equivalents to the pool of plastid thioredoxins (TRXs), via ferredoxin (FDX) and the FDX-dependent TRX reductase (FTR). Alternatively, NADPH is regenerated from FDX by the action of FDX-NADP reductase (FNR). Photosynthesis inevitably produces hydrogen peroxide (H_2O_2), which is scavenged by thiol-dependent peroxidases such as 2-Cys peroxiredoxins (PRXs), PRX Q and glutathione peroxidases (GPXs). 2-Cys PRXs are predominantly reduced by NADPH-dependent thioredoxin reductase C (NTRC), and, to a lesser extent (dashed arrows), by typical (*m*, *f* and *x*) TRXs whereas GPXs are efficiently reduced by TRXs *y*, which also reduces PRX Q (grey arrows). During the day, typical *m*-, *f*- and *x*- TRX types maintain downstream targets reduced, *i.e.* active, the activity of NTRC avoiding the drainage of reducing equivalents from TRXs to 2-Cys PRXs (green pathway). During the night, targets become oxidized, *i.e.*, inactive, as atypical TRXs (TRXL2 and ACHTs) mediate the transfer of their reducing equivalents to 2-Cys PRXs (red pathway). In addition to 2-Cys PRXs, GPXs participate in the dark-oxidation of specific targets, at least RCA and γATPase, most probably through TRXs *y*, which are their most efficient reductant (grey pathway). The redox state of GPXs is not maintained by the activity of NTRC. The question mark indicates the lack of knowledge of specific TRX *y* targets.

glutaredoxin (GRX) rather than by TRXs [62,63]; moreover, the interaction of PRX IIE with 14-3-3 proteins suggests that the role of this PRX in redox signaling is unrelated with its peroxidase activity [62]. In contrast with 2-Cys PRXs, the effect of GPXs is independent of NTRC, as suggested by the similar phenotypes of the *ntrc* and *ntrc-gpx1gpx7* mutants (Fig. 5A, C, D; Figs. S1A–C), and the inability of NTRC to reduce GPXs 1 and 7 (Fig. 6A and B). Since the most efficient reductant of chloroplast GPXs is TRX *y*2 (Fig. 6C), as previously reported for the poplar enzyme [22], the effect of GPXs on chloroplast performance is likely exerted via these TRXs. In this regard, it is worth noting that in contrast with the severe phenotypes of the *ntrc-trxf1f2* and *ntrc-trxx* mutants [59], the *ntrc-trxy1y2* mutant shows a phenotype like the *ntrc* mutant [31]. Altogether, these results suggest that TRXs *y* are not controlled by the NTRC-2-Cys PRXs, but rather by GPXs (Fig. 8, grey pathway).

Funding

This work was supported by Grant PID2020-115156 GB-I00 funded by Ministerio de Ciencia e Innovación/Agencia Estatal de Investigación/10.13039/501100011033. A.C. was supported by a FPU pre-doctoral contract (FPU18-03035) from Ministerio de Universidades (Spain).

Declaration of competing interest

The authors have delcared that there is no conflict of interest.

Data availability

Data will be made available on request.

Acknowledgements

The critical reading of the manuscript by Dr. Naranjo (Instituto de Bioquímica Vegetal y Fotosíntesis, Spain) is deeply appreciated. The anti-RCA antibody was kindly provided by Dr. Portis (USDA, Urbana, USA).

Appendix A. Supplementary data

Supplementary data to this article can be found online at https://doi.org/10.1016/j.redox.2023.102731.

References

[1] S. Khorobrykh, V. Havurinne, H. Mattila, E. Tyystjarvi, Oxygen and ROS in photosynthesis, Plants 9 (2020) 1, https://doi.org/10.3390/plants9010091.
[2] F.J. Schmitt, et al., Reactive oxygen species: re-evaluation of generation, monitoring and role in stress-signaling in phototrophic organisms, Biochim. Biophys. Acta 1837 (2014) 835–848, https://doi.org/10.1016/j.bbabio.2014.02.005.
[3] C. Waszczak, M. Carmody, J. Kangasjarvi, Reactive oxygen species in plant signaling, Annu. Rev. Plant Biol. 69 (2018) 209–236, https://doi.org/10.1146/annurev-arplant-042817-040322.
[4] I. Serrano, M.C. Romero-Puertas, L.M. Sandalio, A. Olmedilla, The role of reactive oxygen species and nitric oxide in programmed cell death associated with self-incompatibility, J. Exp. Bot. 66 (2015) 2869–2876, https://doi.org/10.1093/jxb/erv083.
[5] R. Mittler, ROS are good, Trends Plant Sci. 22 (2017) 11–19, https://doi.org/10.1016/j.tplants.2016.08.002.
[6] R. Mittler, S.I. Zandalinas, Y. Fichman, F. Van Breusegem, Reactive oxygen species signalling in plant stress responses, Nat. Rev. Mol. Cell Biol. 23 (2022) 663–679, https://doi.org/10.1038/s41580-022-00499-2.
[7] A. Mhamdi, F. Van Breusegem, Reactive oxygen species in plant development, Development 145 (2018) 15, https://doi.org/10.1242/dev.164376.
[8] F.K. Choudhury, R.M. Rivero, E. Blumwald, R. Mittler, Reactive oxygen species, abiotic stress and stress combination, Plant J. 90 (2017) 856–867, https://doi.org/10.1111/tpj.13299.
[9] A. Pinnola, R. Bassi, Molecular mechanisms involved in plant photoprotection, Biochem. Soc. Trans. 46 (2018) 467–482, https://doi.org/10.1042/BST20170307.
[10] M. Pilon, K. Ravet, W. Tapken, The biogenesis and physiological function of chloroplast superoxide dismutases, Biochim. Biophys. Acta 1807 (2011) 989–998, https://doi.org/10.1016/j.bbabio.2010.11.002.
[11] K. Bela, R. Riyazuddin, J. Csiszar, Plant glutathione peroxidases: non-heme peroxidases with large functional flexibility as a core component of ROS-processing mechanisms and signalling, Antioxidants 11 (2022) 8, https://doi.org/10.3390/antiox11081624.
[12] K.-J. Dietz, Thiol-based peroxidases and ascorbate peroxidases: why plants rely on multiple peroxidase systems in the photosynthesizing chloroplast? Mol. Cell 39 (2016) 20–25, https://doi.org/10.14348/molcells.2016.2324.
[13] G. Passaia, M. Margis-Pinheiro, Glutathione peroxidases as redox sensor proteins in plant cells, Plant Sci. 234 (2015) 22–26, https://doi.org/10.1016/j.plantsci.2015.01.017.
[14] L. Vogelsang, K.-J. Dietz, Plant thiol peroxidases as redox sensors and signal transducers in abiotic stress acclimation, Free Radic. Biol. Med. 193 (2022) 764–778, https://doi.org/10.1016/j.freeradbiomed.2022.11.019.
[15] K.-J. Dietz, Peroxiredoxins in plants and cyanobacteria, Antioxidants Redox Signal. 15 (2011) 1129–1159, https://doi.org/10.1089/ars.2010.3657.
[16] M. Liebthal, D. Maynard, K.-J. Dietz, Peroxiredoxins and redox signaling in plants, Antioxidants Redox Signal. 28 (2018) 609–624, https://doi.org/10.1089/ars.2017.7164.
[17] E.S. Lee, C.H. Kang, J.H. Park, S.Y. Lee, Physiological significance of plant peroxiredoxins and the structure-related and multifunctional biochemistry of peroxiredoxin 1, Antioxidants Redox Signal. 28 (2018) 625–639, https://doi.org/10.1089/ars.2017.7400.
[18] J.B. Peltier, et al., The oligomeric stromal proteome of *Arabidopsis thaliana* chloroplasts, Mol. Cell. Proteomics 5 (2006) 114–133, https://doi.org/10.1074/mcp.M500180-MCP200.
[19] K. Bela, E. Horvath, A. Galle, L. Szabados, I. Tari, J. Csiszar, Plant glutathione peroxidases: emerging role of the antioxidant enzymes in plant development and stress responses, J. Plant Physiol. 176 (2015) 192–201, https://doi.org/10.1016/j.jplph.2014.12.014.
[20] M.A. Rodriguez Milla, A. Maurer, A. Rodriguez Huete, J.P. Gustafson, Glutathione peroxidase genes in Arabidopsis are ubiquitous and regulated by abiotic stresses through diverse signaling pathways, Plant J. 36 (2003) 602–615, https://doi.org/10.1046/j.1365-313x.2003.01901.x.
[21] A. Iqbal, Y. Yabuta, T. Takeda, Y. Nakano, S. Shigeoka, Hydroperoxide reduction by thioredoxin-specific glutathione peroxidase isoenzymes of *Arabidopsis thaliana*, FEBS J. 273 (2006) 5589–5597, https://doi.org/10.1111/j.1742-4658.2006.05548.x.
[22] N. Navrot, et al., Plant glutathione peroxidases are functional peroxiredoxins distributed in several subcellular compartments and regulated during biotic and abiotic stresses, Plant Physiol. 142 (2006) 1364–1379, https://doi.org/10.1104/pp.106.089458.
[23] K. Chibani, B. Pucker, K.-J. Dietz, A. Cavanagh, Genome-wide analysis and transcriptional regulation of the typical and atypical thioredoxins in *Arabidopsis thaliana*, FEBS Lett. 595 (2021) 2715–2730, https://doi.org/10.1002/1873-3468.14197.
[24] P. Geigenberger, I. Thormählen, D.M. Daloso, A.R. Fernie, The unprecedented versatility of the plant thioredoxin system, Trends Plant Sci. 22 (2017) 249–262, https://doi.org/10.1016/j.tplants.2016.12.008.
[25] Z. Kang, T. Qin, Z. Zhao, Thioredoxins and thioredoxin reductase in chloroplasts: a review, Gene 706 (2019) 32–42, https://doi.org/10.1016/j.gene.2019.04.041.
[26] Y. Meyer, C. Belin, V. Delorme-Hinoux, J.P. Reichheld, C. Riondet, Thioredoxin and glutaredoxin systems in plants: molecular mechanisms, crosstalks, and functional significance, Antioxidants Redox Signal. 17 (2012) 1124–1160, https://doi.org/10.1089/ars.2011.4327.
[27] L. Nikkänen, J. Toivola, M.G. Díaz, E. Rintamäki, Chloroplast thioredoxin systems: prospects for improving photosynthesis, Phil. Trans. Royal Soc. 372 (2017) 1730, https://doi.org/10.1098/rstb.2016.0474.
[28] M. Zaffagnini, et al., Redox homeostasis in photosynthetic organisms: novel and established thiol-based molecular mechanisms, Antioxidants Redox Signal. 31 (2019) 155–210, https://doi.org/10.1089/ars.2018.7617.
[29] V. Collin, et al., The Arabidopsis plastidial thioredoxins: new functions and new insights into specificity, J. Biol. Chem. 278 (2003) 23747–23752, https://doi.org/10.1074/jbc.M302077200.
[30] V. Collin, et al., Characterization of plastidial thioredoxins from Arabidopsis belonging to the new y-type, Plant Physiol. 136 (2004) 4088–4095, https://doi.org/10.1104/pp.104.052233.
[31] A. Jurado-Flores, et al., Exploring the functional relationship between y-type thioredoxins and 2-Cys peroxiredoxins in Arabidopsis chloroplasts, Antioxidants 9 (2020) 1072, https://doi.org/10.3390/antiox9111072, 2020.
[32] K. Yoshida, A. Hara, K. Sugiura, Y. Fukaya, T. Hisabori, Thioredoxin-like2/2-Cys peroxiredoxin redox cascade supports oxidative thiol modulation in chloroplasts, Proc. Natl. Acad. Sci. USA 115 (2018) E8296–E8304, https://doi.org/10.1073/pnas.1808284115.
[33] M. Broin, S. Cuine, F. Eymery, P. Rey, The plastidic 2-Cysteine peroxiredoxin is a target for a thioredoxin involved in the protection of the photosynthetic apparatus against oxidative damage, Plant Cell 14 (2002) 1417–1432, https://doi.org/10.1105/tpc.001644.
[34] I. Dangoor, H. Peled-Zehavi, G. Wittenberg, A. Danon, A chloroplast light-regulated oxidative sensor for moderate light intensity in Arabidopsis, Plant Cell 24 (2012) 1894–1906, https://doi.org/10.1105/tpc.112.097139.
[35] E. Eliyahu, I. Rog, D. Inbal, A. Danon, ACHT4-driven oxidation of APS1 attenuates starch synthesis under low light intensity in Arabidopsis plants, Proc. Natl. Acad. Sci. USA 112 (2015) 12876–12881, https://doi.org/10.1073/pnas.1515513112.
[36] F. Alkhalfioui, M. Renard, F. Montrichard, Unique properties of NADP-thioredoxin reductase C in legumes, J. Exp. Bot. 58 (2007) 969–978, https://doi.org/10.1093/jxb/erl248.
[37] J.C. Moon, et al., The C-type Arabidopsis thioredoxin reductase ANTR-C acts as an electron donor to 2-Cys peroxiredoxins in chloroplasts, Biochem. Biophys. Res. Commun. 348 (2006) 478–484, https://doi.org/10.1016/j.bbrc.2006.07.088.
[38] J.M. Pérez-Ruiz, et al., Rice NTRC is a high-efficiency redox system for chloroplast protection against oxidative damage, Plant Cell 18 (2006) 2356–2368, https://doi.org/10.1105/tpc.106.041541.
[39] P. Pulido, et al., Functional analysis of the pathways for 2-Cys peroxiredoxin reduction in *Arabidopsis thaliana* chloroplasts, J. Exp. Bot. 61 (2010) 4043–4054, https://doi.org/10.1093/jxb/erq218.
[40] J.M. Pérez-Ruiz, B. Naranjo, V. Ojeda, M. Guinea, F.J. Cejudo, NTRC-dependent redox balance of 2-Cys peroxiredoxins is needed for optimal function of the photosynthetic apparatus, Proc. Natl. Acad. Sci. USA 114 (2017) 12069–12074, https://doi.org/10.1073/pnas.1706003114.
[41] V. Ojeda, J.M. Pérez-Ruiz, F.J. Cejudo, 2-Cys peroxiredoxins participate in the oxidation of chloroplast enzymes in the dark, Mol. Plant 11 (2018) 1377–1388, https://doi.org/10.1016/j.molp.2018.09.005.
[42] M.J. Vaseghi, et al., The chloroplast 2-Cysteine peroxiredoxin functions as thioredoxin oxidase in redox regulation of chloroplast metabolism, Elife 7 (2018), https://doi.org/10.7554/eLife.38194.
[43] Y. Yokochi, Y. Fukushi, K.I. Wakabayashi, K. Yoshida, T. Hisabori, Oxidative regulation of chloroplast enzymes by thioredoxin and thioredoxin-like proteins in *Arabidopsis thaliana*, Proc. Natl. Acad. Sci. USA 118 (2021), e2114952118, https://doi.org/10.1073/pnas.2114952118.
[44] N. Lampl, et al., Systematic monitoring of 2-Cys peroxiredoxin-derived redox signals unveiled its role in attenuating carbon assimilation rate, Proc. Natl. Acad. Sci. USA 119 (2022), e2119719119, https://doi.org/10.1073/pnas.2119719119.
[45] A.J. Serrato, J.M. Pérez-Ruiz, M.C. Spínola, F.J. Cejudo, A novel NADPH thioredoxin reductase, localized in the chloroplast, which deficiency causes hypersensitivity to abiotic stress in *Arabidopsis thaliana*, J. Biol. Chem. 279 (2004) 43821–43827, https://doi.org/10.1074/jbc.M404696200.
[46] V. Ojeda, J. Jiménez-López, F.J. Romero-Campero, F.J. Cejudo, J.M. Perez-Ruiz, A chloroplast redox relay adapts plastid metabolism to light and affects cytosolic protein quality control, Plant Physiol. 187 (2021) 88–102, https://doi.org/10.1093/plphys/kiab246.
[47] D.M. Kramer, G. Johnson, O. Kiirats, G.E. Edwards, New fluorescence parameters for the determination of q(a) redox state and excitation energy fluxes, Photosynth. Res. 79 (2004) 209–218, https://doi.org/10.1023/B:PRES.0000015391.99477.0d.
[48] G. Passaia, G. Queval, J. Bai, M. Margis-Pinheiro, C.H. Foyer, The effects of redox controls mediated by glutathione peroxidases on root architecture in *Arabidopsis thaliana*, J. Exp. Bot. 65 (2014) 1403–1413, https://doi.org/10.1093/jxb/ert486.
[49] S. Attacha, et al., Glutathione peroxidase-like enzymes cover five distinct cell compartments and membrane surfaces in *Arabidopsis thaliana*, Plant Cell Environ. 40 (2017) 1281–1295, https://doi.org/10.1111/pce.12919.
[50] K. Li, et al., The chlorophyll fluorescence 244 (HCF244) is potentially involved in glutathione peroxidase 7-regulated light stress in *Arabidopsis thaliana*, Environ. Exp. Bot. 195 (2022), 104767, https://doi.org/10.1016/j.envexpbot.2021.104767.

[51] C.C. Chang, et al., Arabidopsis chloroplastic glutathione peroxidases play a role in cross talk between photooxidative stress and immune responses, Plant Physiol. 150 (2009) 670–683, https://doi.org/10.1104/pp.109.135566.
[52] K. Bela, et al., Comprehensive analysis of antioxidant mechanisms in Arabidopsis glutathione peroxidase-like mutants under salt- and osmotic stress reveals organ-specific significance of the AtGPXL's activities, Environ. Exp. Bot. 157 (2018) 127–140, https://doi.org/10.1016/j.envexpbot.2018.02.016.
[53] B.B. Buchanan, The path to thioredoxin and redox regulation in chloroplasts, Annu. Rev. Plant Biol. 67 (2016) 1–24, https://doi.org/10.1146/annurev-arplant-043015-111949.
[54] F.J. Cejudo, M.C. González, J.M. Pérez-Ruiz, Redox regulation of chloroplast metabolism, Plant Physiol. 186 (2021) 9–21, https://doi.org/10.1093/plphys/kiaa062.
[55] L. Michelet, et al., Redox regulation of the Calvin-Benson cycle: something old, something new, Front. Plant Sci. 4 (2013) 470, https://doi.org/10.3389/fpls.2013.00470.
[56] P. Schürmann, B.B. Buchanan, The ferredoxin/thioredoxin system of oxygenic photosynthesis, Antioxidants Redox Signal. 10 (2014) 1235–1274, https://doi.org/10.1089/ars.2007.1931.
[57] A. Lepistö, et al., Chloroplast NADPH-thioredoxin reductase interacts with photoperiodic development in Arabidopsis, Plant Physiol. 149 (2009) 1261–1276, https://doi.org/10.1104/pp.108.133777.
[58] J. Awad, et al., 2-Cysteine peroxiredoxins and thylakoid ascorbate peroxidase create a water-water cycle that is essential to protect the photosynthetic apparatus under high light stress conditions, Plant Physiol. 167 (2015) 1592–1603, https://doi.org/10.1104/pp.114.255356.
[59] V. Ojeda, et al., NADPH thioredoxin reductase C and thioredoxins act concertedly in seedling development, Plant Physiol. 174 (2017) 1436–1448, https://doi.org/10.1104/pp.17.00481, 2017.
[60] I. Thormählen, et al., Thioredoxin f1 and NADPH-dependent thioredoxin reductase C have overlapping functions in regulating photosynthetic metabolism and plant growth in response to varying light conditions, Plant Physiol. 169 (2015) 1766–1786, https://doi.org/10.1104/pp.15.01122.
[61] V. Ojeda, J.M. Pérez-Ruiz, F.J. Cejudo, The NADPH-dependent thioredoxin reductase C-2-Cys peroxiredoxin redox system modulates the activity of thioredoxin x in Arabidopsis chloroplasts, Plant Cell Physiol. 59 (2018) 2155–2164, https://doi.org/10.1093/pcp/pcy134.
[62] A. Dreyer, et al., Function and regulation of chloroplast peroxiredoxin IIE, Antioxidants 10 (2021) 2, https://doi.org/10.3390/antiox10020152.
[63] F. Gama, et al., Functional analysis and expression characteristics of chloroplastic Prx IIE, Physiol. Plantarum 133 (2008) 599–610, https://doi.org/10.1111/j.1399-3054.2008.01097.x.